Ab Initio Study of The Properties of The Chalcopyrites $AgInS_2$, $AgInSe_2$ and $AgInTe_2$

[1]Omehe N. N., and [2]Ehika S.

[1]Federal University, Otuoke, Bayelsa State, Nigeria.

[2]Ambrose Alli University, Ekpoma, Edo state, Nigeria.

ehikasimon@yahoo.com

Abstract:

$AgInS_2$, $AgInSe_2$ and $AgInTe_2$ are materials with Chalcopyrite structure whose properties have been studied using the pseudopotential method within the density functional theory (DFT) framework. The LDA+U scheme together with the projector augmented wave (PAW) were used for the electronic band structure calculations, while the norm-conserving pseudopotentials were used for the structural optimizations. The results of the investigations predicted the materials $AgInS_2$, $AgInSe_2$ and $AgInTe_2$ to be semiconductors with energy band gap value of 1.77 eV, 1.63 eV and 1.29 eV respectively. The total density of states and their corresponding partial density of states were also computed. The In-s state was the dominant state in the conduction band for all the materials while the S-p, Se-p and Te-p states dominated the valence band preceding the Fermi level.

Keywords*:* Silver Indium disulpgide ($AgInS_2$), Silver Indium diselenide ($AgInSe_2$), Silver Indium ditelluride ($AgInTe_2$), Electronic band structure of Silver Indium disulpgide ($AgInS_2$), Chalcopyrites materials

INTRODUCTION

This group of compounds have the chalcopyrite structure to which the crystals $AgInS_2$, $AgInSe_2$ and $AgInTe_2$ are members. Chalcopyrite has a relativity simple structure of the ZnS type and also a diamond lattice. It`s a tetragonal crystal system constructed from sulphur S (or Selenium Se or Tellurium Te) atoms surrounded by two Silver (Ag) atoms and two Indium (In) atoms each at the corners of a nearly regular tetrahedron. These materials have attracted considerable amount of attention from both theoretical and experimental researchers due to their technological applications. These materials have found applications in the fields of photovoltaic cells, photo catalysis, optoelectronics designing of non-linear optical devices, solar cells optical detectors and light emitting diode (LED) (Kopytov and Kosobutsky, 2010; Baeissa, 2014; Yin et al, 2013; Xue et al, 2000)

Experimentally, quite a number of researchers have worked on these materials. The Single Source Thermal Evaporation Method (Akaki et al, 2005; Khudayer et al, 2018; Lee et al, 2007); Far Infrared Reflectivity and Optical Absorption (Koitabashi et al, 2010). Also, the co-evaporation method was employed to investigate $AgInSe_2$ (Kumar and Pradeep, 2009; Arredondo and Gordillo, 2010); the ultra-high vacuum pulsed laser deposition method was used by Mustafa et al (2007); Molecular beam epitaxial Method (Yamada et al 2006; Martins and Pamela (2005). Furthermore, Vertical gradient temperature freezing Method was employed by Yoshino et al, (2001); Solid state microwave irradiation (Tadjarodi and Cheshmekhavar 2012); Electrodeposition technique (Kulkarni, 2016; Aouaj et al, 2015); Sol-gel spin-coating technique grown on Si substrate (Al-Agel and Mahmoud (2012); Chemical bath deposition (CBD) (Chang et al, 2010) and Facile route (Ranjbar et al, 2014).

Theoretically, these materials have received attention. Kopytov and Kosobutsky (2010), worked on the thermodynamic and elastic properties of $AgInSe_2$ and $AgInTe_2$. Also, Zhang et al (2014) investigated the structure and thermal properties of $AgInTe_2$ using the pseudopotential method with the ultra-soft pseudopotential. Nguimdo et al (2016) studied the structure and electronic properties of the ternary compound $AgInS_2$. They did a comparative study of the effect of different functional on the energy band gap, and reported a band gap range of 0.27 to 1.73 eV. Sharma et al (2014) carried out a first principle study on the structural, electronic, optical, elastic and thermal properties of $AgInX_2$ (X=S, Se). They employed the full potential linearized augmented plane wave, and reported a deformation parameter u for $AgInS_2$ and $AgInSe_2$ to be 0.261 and 0.265 respectively. Kotmool et al (2015) did a theoretical study of structural phase transformation and band structure of AgInTe2 under high pressure based on DFT within both local density approximation (LDA) and generalised gradient approximation (GGA) exchange-correlation, and reported band gap values of 1.02 eV and 0.95 eV for GGA and LDA functional respectively.

In this study, the pseudopotential method will be used in conjunction with the LDA+U scheme to investigate the electronic properties of $AgInS_2$, $AgInSe_2$ and $AgInTe_2$.

COMPUTATIONAL DETAIL

The ternary Chalcopyrites belongs to the space group (space group number 122). The Chalcopyrite structure is a superlattice of the Zinc-blende structure. The I-III-VI_2 chalcopyrite has each group VI member [Sulphur (S), Selenium (S), Tellurium Te] coordinated by two group I [Silver (Ag)] and two group III atoms [Indium (In)]. Each group III atom is tetrahedrally coordinated by four group VI atoms. In and Ag are at the 4a and 4b Wyckoff's atomic positions respectively. S or Se or Te is at the 8d site as the case may be. The z value for the materials is four (4), which gives a total of 16 atomic coordinates of three (3) types. Here, structure optimization and electronic band structure were performed for $AgInS_2$, $AgInSe_2$ and $AgInTe_2$. The pseudopotential method was used within the density functional theory (DFT) framework. The Abinit (Gonze et al, 2002; Gonze et al, 2005) Quantum suite of packages was used in this study. In the structural optimization of the materials under investigations, the starting lattice parameters were adopted from the experimental value (Madelung, 2001). The x component of the 8d Wyckoff's position was allowed to evolve while the others were fixed. The self-consistency iterations continued until a force tolerance of 0.01 was reached. The optimization was done without the LDA+U component of the Abinit package. The result of the optimizations is shown in Table 1. For the energy bands, total density of states (DOS), partial density of states (PDOS) and charge transfer. The LDA+U scheme was used with the projector augmented wave as implemented in the Abinit package. The following were states included in the computations: Ag has the 4s, 4p,4d and 5s orbitals, In has 5s, 5p while S, Se and Te were represented by 3s,3p; 4s, 4p and 5s, 5p states respectively. The plane waves were generated by a kenetic energy cut-off of 10 Ha, a Monkhorst-Pack shifted grid 4x4x4 yielding a mesh of 256 k-ponit, which was used for the Brillioun zone intergration. The self-consistent computation was deemed to have achieved convergence when the energy tolerance of 10^{-8} was reached.

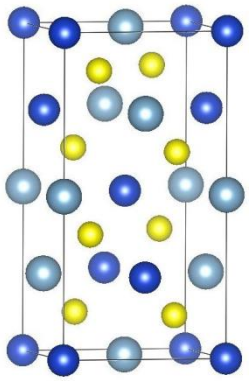

Fig. 1: The structure used in the computations. Yellow balls represent S or Se or Te atoms, Blue balls for Ag atoms and Grey for In atoms.

Table 1: Optimization results

	a()	c()	*x*	*y*	*z*
$AgInS_2$	5.7873	11.1073	0.0	0.0	0.0
			0.0	0.0	0.5
			u=0.19	0.25	0.125
Experiment	5.82[a], 5.80[c], 5.807[d], 5.816[e],	11.17[a], 11.33[c], 11.85[d], 11.17[e],	u=261[b], 0.25[c]		
$AgInSe_2$	6.0527	11.6088	0.0	0.0	0.0
			0.0	0.0	0.5

			u=0.212	0.25	0.125
Experiment	6.095[a], 6.086[d], 6.102[f,g]	11.69[a], 11.80[d], 11.69[f,g],	u=0.265[b],		
$AgInTe_2$	6.4287	12.5875	0.0	0.0	0.0
			0.0	0.0	0.5
			u=0.194	0.25	0.125
Experiment	6.43[a], 6.35[d]	12.59[a], 12.6531[d]	0.26[d]		

[a]Madelung (2001)

[b]Sharma et al (2014)

[c]Nguimado et al (2015)

[d]Zhang et al (2014)

[e]Ranjbar et al (2014)

[f]Lee et al (2007)

[g]Al-Agel and Mahmmoud (2012)

RESULTS AND DISCUSSIONS

Figures 2a to 2c show the electronic band structure of the materials under investigation, that is, $AgInS_2$, $AgInSe_2$ and $AgInTe_2$ respectively. The band structure is a plot of energy against high symmetry points, that is, the first brillioun zone. The dashed lines indicate the Fermi energy. Figure 2 shows that the valence band maximum (VBM) and the conduction band minimum (CBM) are both along the gamma point. The valence bands show narrow dispersion, while the bands around the Fermi level are flat. This might indicate that transitions from all high symmetry points are notable. There is a slight decrease in band energy from the Fermi level at the M point of high symmetry from $AgInS_2$ to $AgInTe_2$ as seen from Fig 2. Computational results presented in Fig 2 indicate that the materials $AgInS_2$, $AgInSe_2$ and $AgInTe_2$ are semiconductors. The optical bands gaps of these materials are 1.77 eV, 1.63 eV and 1.29 eV for $AgInS_2$, $AgInSe_2$ and $AgInTe_2$ respectively. These results are in excellent agreement with experimental and other theoretical results. The experimental band gap value of $AgInS_2$ reported by Chang et al (2010) ranges from 1.873 eV to 1.92 eV, while Madelung (2001) reported a range of value from 1.87 eV to 2.02 eV. Sharma et al (2014) reported a theoretical value of 1.61 eV, Nguimdo et al (2015) obtained a range of value from 0.27 eV to 1.73 eV. The experimental value reported for $AgInSe_2$ by Madelung (2001) ranges from 1.24 to 1.6 eV. On the other hand, Koitabashi et al (2010) reported a value of 1.2 eV; Aouaj et al (2015) reported a band gap value of 1.24 e3V; Khudager et al (2016) reported a range of value from 1.6 eV to 1.9 eV; Lee et al (2007) obtained a range of value of 1.76 eV to 1.82 eV and Sharma et al (2014) reported a computed value of 1.24 eV.

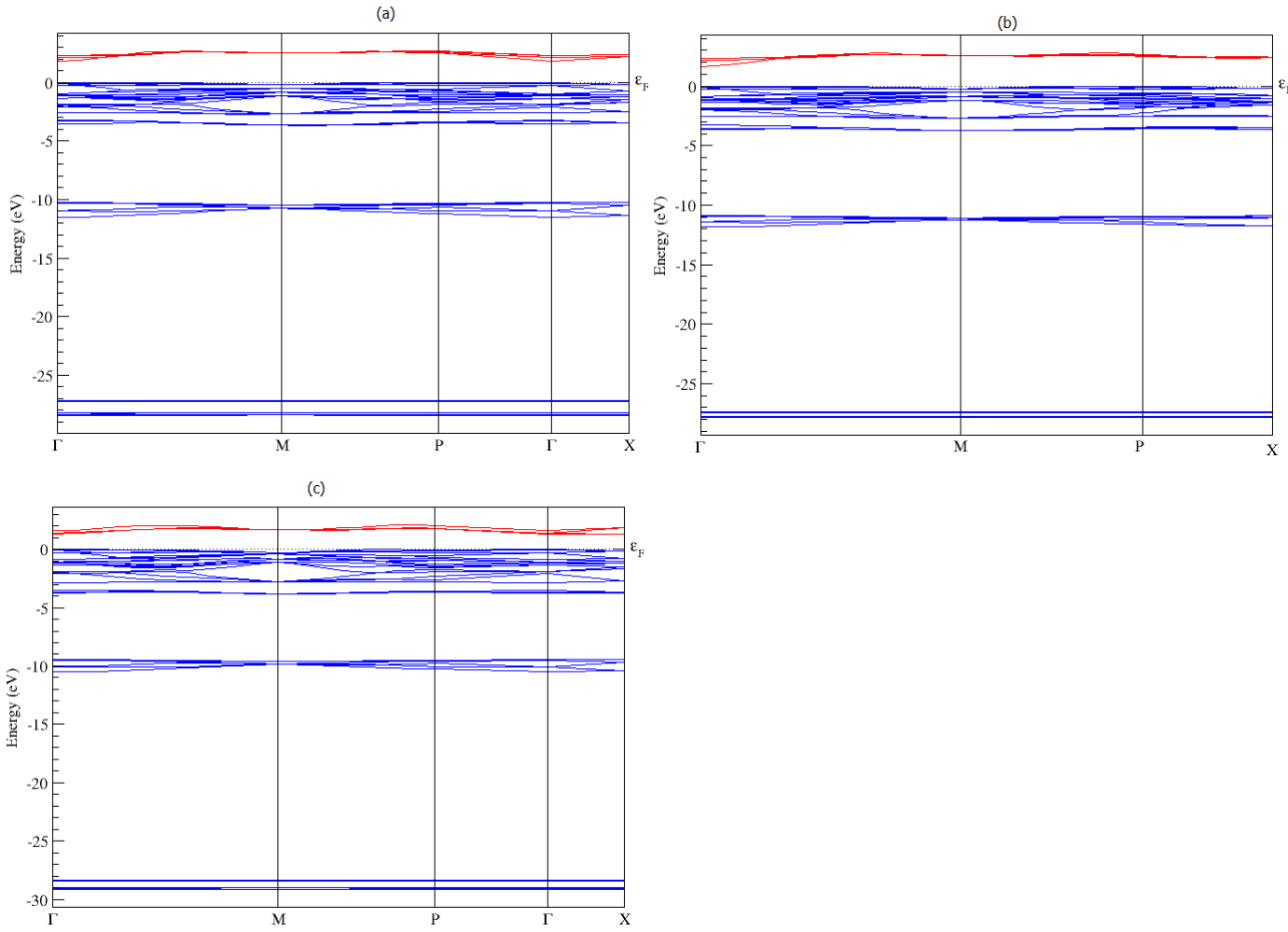

Fig. 2: The electronic band structure of (a) $AgInS_2$ (b) $AgInSe_2$ (c) $AgInTe_2$. E_F indicate the Fermi level.

The experimental value reported for $AgInTe_2$ in the literature by Madelung is 0.964 eV, Kotmool et al reported a calculated value of between 0.95 eV and 1.02 eV. The total density of states (TDOS) for the materials $AgInS_2$, $AgInSe_2$ and $AgInTe_2$ are presented in Figs. 3a to 3c respectively, and the plot is DOS versus energy in Hartree. All the features of the band structure plots are well reproduced in the TDOS graph. The band gaps are clearly seen at the Fermi level of the TDOS plot, re-emphasizing the semiconducting nature of these materials. The various peaks and curves in the TDOS graphs in Fig 3 correspond to the different sections of the band structure (Fig 2). For example, $AgInS_2$ represented by Fig 3a presents about six (6) peaks or curves separated by different energy values. These curves correspond to the 6 sections into which its band structure (Fig 2a) is parted.

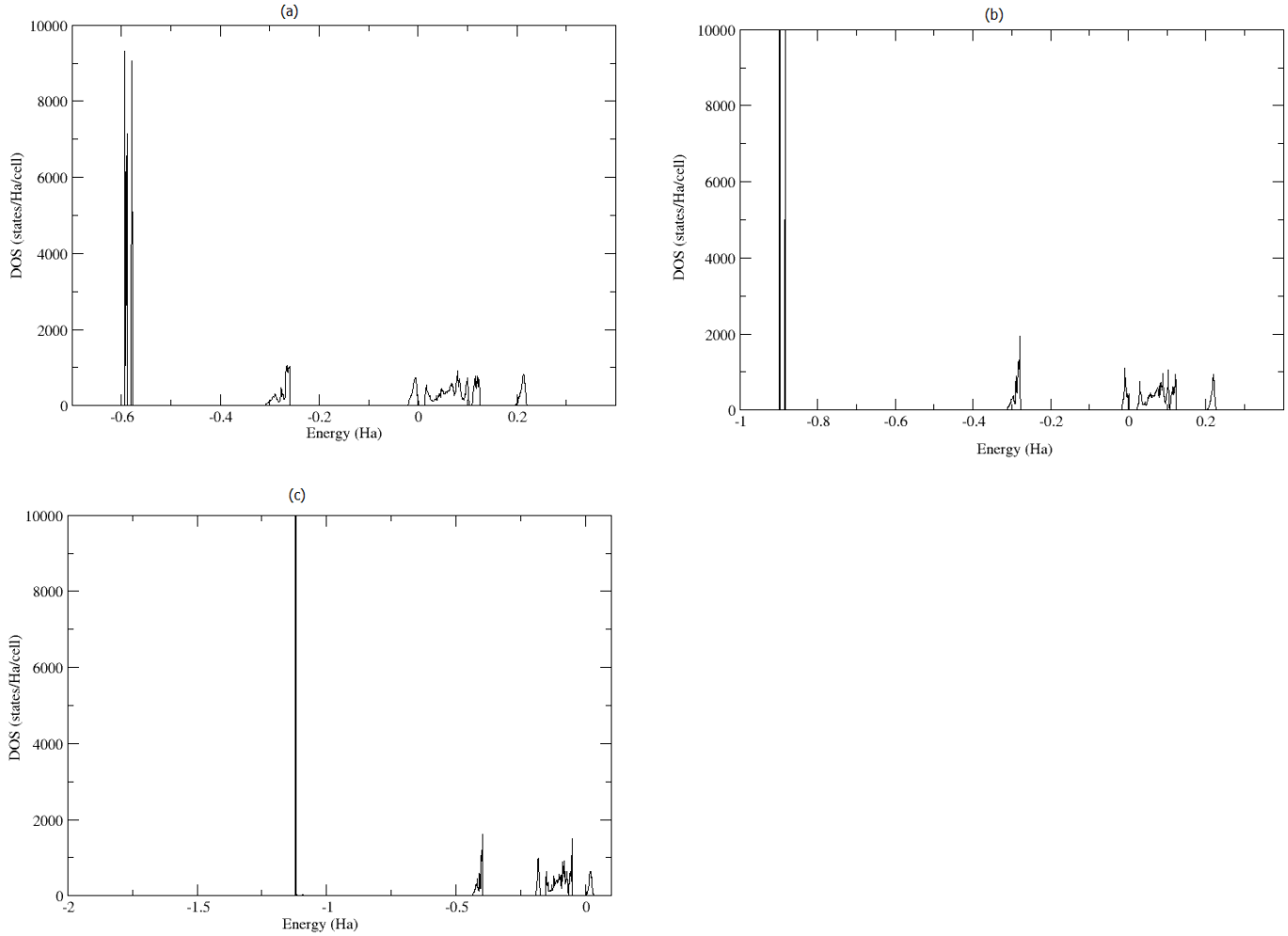

Fig. 3: Total density of states for (a) $AgInS_2$ with the Fermi level at 0.13 Ha (b) $AgInSe_2$ with the Fermi level at 0.12 Ha (c) $AgInTe_2$ with the Fermi level at – 0.05 Ha

The partial density of states (PDOS), that is, the orbital components to the density of states of the materials under investigation are presented in Figs 4 to 6 for $AgInS_2$, $AgInSe_2$ and $AgInTe_2$ respectively. The states included as valence in the pseudopotential computations are Ag: 4d, 5s; In: 5s, 5p; Te: 5s, 5p. The orbital decomposition of the TDOS of $AgInS_2$ is presented in Fig 4. The Ag-d states are dominant about -0.6 Ha as seen from Fig 4a. About the zero mark on the energy axis, it can be seen from Fig 4b that The In-s state is dominant, and is also mostly made up of the conduction band. Figure 4c shows that the states preceding the Fermi level are predominantly made up of the S-p states, while the S-s state is dominant about -0.3 Ha. States also found in the conduction band are the In-p and S-p. Other notable states around the Fermi level are Ag-s, In-p and In-s.

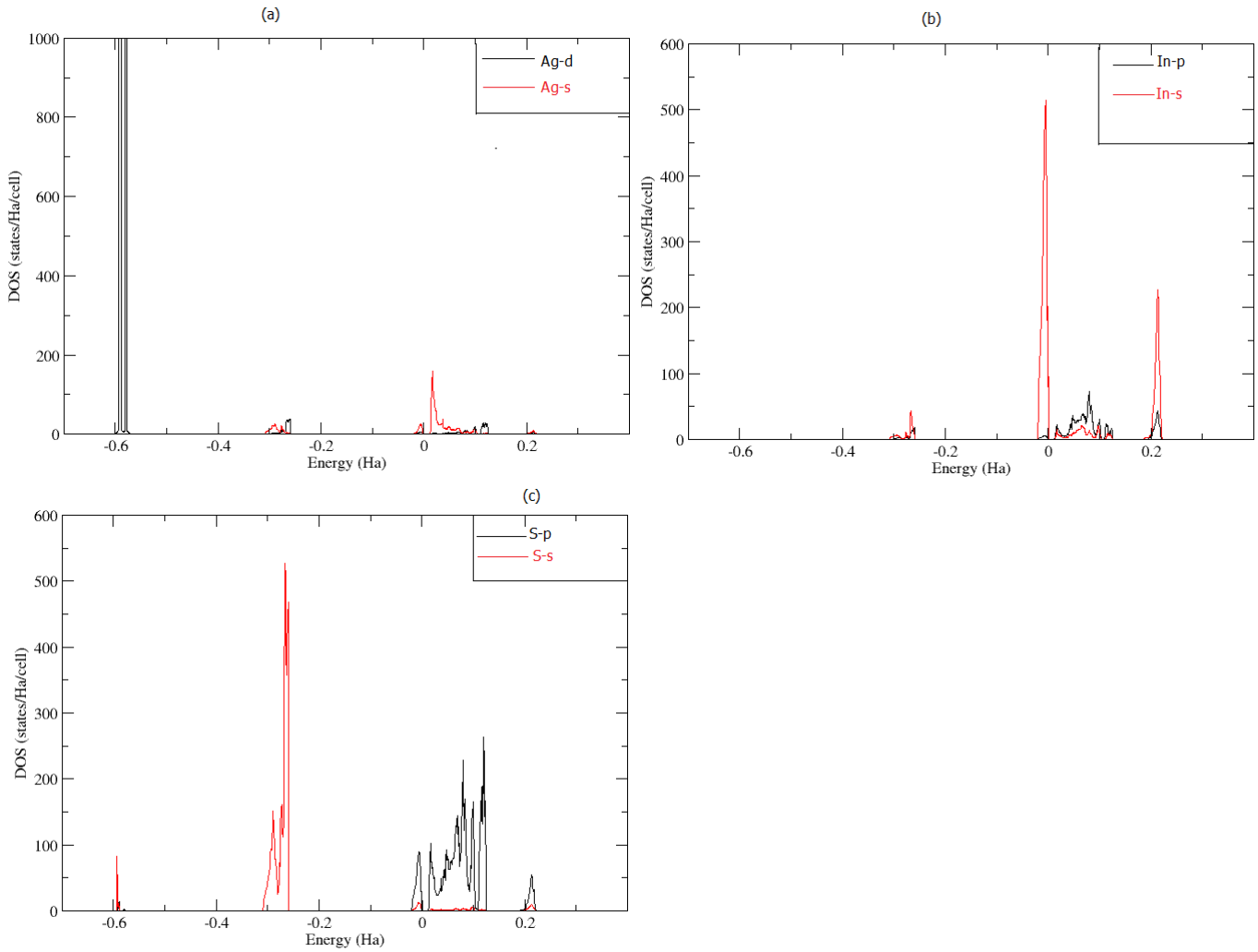

Fig 4: The partial density of states of $AgInS_2$. The Fermi level is at 0.13 Ha. (a) orbital contributions from the Silver Ag atom (b) orbital contributions from the Indium In atom (c) orbital contributions from the Sulphur S atom.

The orbital decomposition of the TDOS of $AgInSe_2$ is presented in Fig 5. Ag-d is least in energy and dominates the far left of the Fig 5a about -0.9 Ha. The In-s states dominate the zero mark as clearly seen in Fig 5b. Again, the In-s state is the dominate state in the conduction band just as in $AgInS_2$. The valence states after the zero mark are made up of Ag-s, In-p and Se-p, while Se-s dominates about -0.3 Ha. Other states in the conduction band apart from the dominant states are the In-p and se-p.

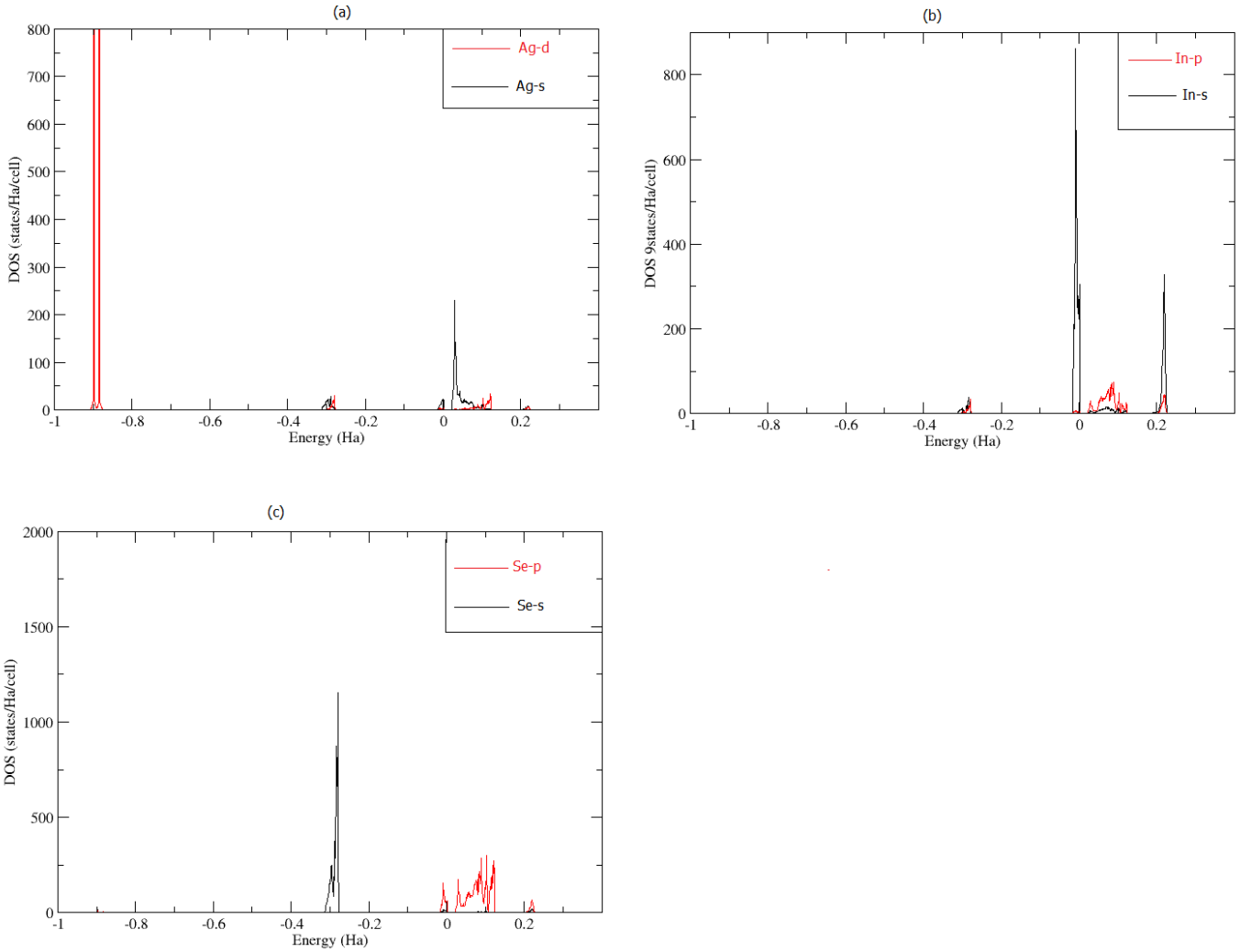

Fig 5: The partial density of states of $AgInSe_2$. The Fermi level is at 0.13 Ha. (a) orbital contributions from the Silver Ag atom (b) orbital contributions from the Indium In atom (c) orbital contributions from the Selenium Se atom.

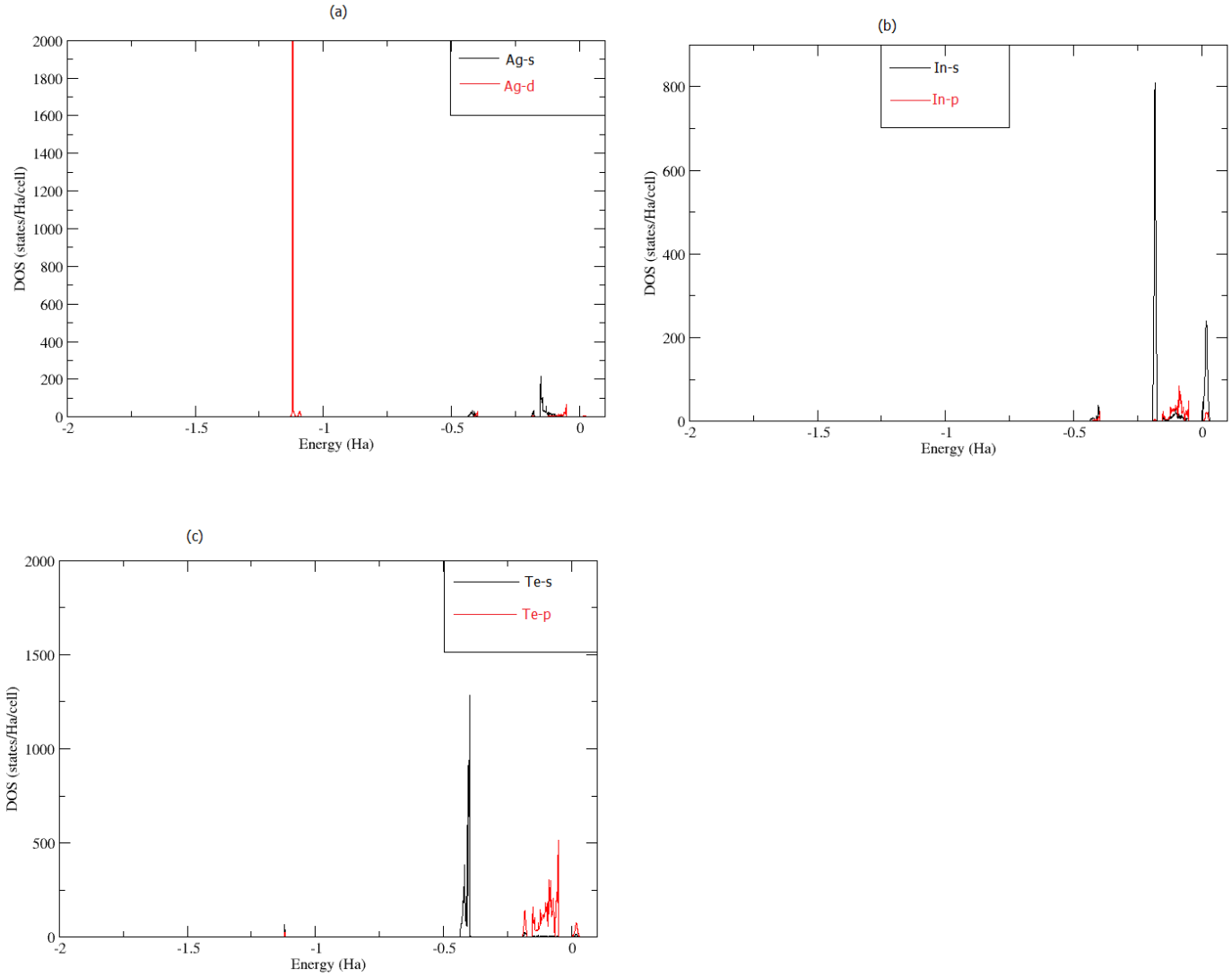

Fig 6: The partial density of states of $AgInTe_2$. The Fermi level is at -0.05 Ha. (a) orbital contributions from the Silver Ag atom (b) orbital contributions from the Indium In atom (c) orbital contributions from the Tellurium Te atom.

The orbital decomposition of the TDOS of $AgInTe_2$ is presented in Fig 6. The peak representing the Ag-d states is very sharp and narrow suggesting a far less dispersion compared to $AgInS_2$ and $AgInSe_2$. Again, as in $AgInS_2$ and $AgInSe_2$, it is less in energy and dominates the far left in Fig 6a. In-s states dominate the zero mark as clearly seen in Fig 5b. The In-s state is the dominate state in the conduction band just as in $AgInS_2$ and $AgInSe_2$. The valence states after the zero mark are made up of Ag-s, In-p and Te-p, while Te-s dominates about -0.4 Ha. Other states in the conduction band apart from the dominant states are the In-p and Te-p.

Conclusion

The electronic band structure, the total density of states and the partial density of states for $AgInS_2$, $AgInSe_2$ and $AgInTe_2$ Chalcopyrite materials have been studied using the pseudopotential method within the density functional theory (DFT) framework. The LDA+U scheme together with the projector augmented wave (PAW) were used for the electronic band structure calculations, while the norm-conserving pseudopotentials were used for the structural optimizations. The results of the investigations predicted the materials $AgInS_2$, $AgInSe_2$ and $AgInTe_2$ to be semiconductors with energy band gap value of 1.77 eV, 1.63 eV and 1.29 eV respectively. The transition points in the band structure are all notable because of the narrowness of the bands about the Fermi level. The total density of states and their corresponding partial density of states were also computed. The In-s

state was the dominate state in the conduction band for all the materials while the S-p, Se-p and Te-p states dominated the valence band preceding the Fermi level.

References

1. Akaki, Y., Kurihara, S., Shirahama, M., Tsurugida, K., Seto, S., Kakeno, T. & Yoshino, K. (2005), Structural, electrical and optical properties of $AgInS_2$ thin films grown by thermal evaporation method J. Phy.Chm. Solid 66, 1858-1861.
2. Al-Agel, F. A. and Mahmoud, W. E. (2012). Synthesis and characterization of highly stoichiometric $AgInSe_2$ thin films *via* a sol–gel spin-coating technique. J. Appl. Cryst. 45, 921-925.
3. Aouaj, A. M., Diaz, R., Moursli, F. C. E., Tiburcio-Silver, A. % Abd-Lefdil, M. (2015), $AgInSe_2$ thin films prepared by Electrodeposition process. Inter. J. of mater. Sci. and Appl. 4 , 35-38.
4. Arredondo, C. A. and Gordillo, G. (2010), Photoconductive and electrical transport properties of AginSe2 thin films prepared by co-evaporation. Phys. B: Cond. Matter 405, 3694-3699.
5. Baeissa, E. (2014). Environmental remediation of thiophene solution by photocatalytic oxidation using NiO/AgInS2 nanoparticles. Journal of Industrial and Engineering Chemistry, l.20, 3270-3275. DOI10.1016/j.jiec.2013.12.008
6. Chang, W-S., Wu, C-C., Jeng, M-S. & Lee, T. H. (2010), Ternary Ag-In-S polycrystalline films deposited using chemical bath deposition for photoelectrochemical applications, mater. Chm and Phys., 120 (2-3), 307-312.
7. Nguimdo, G.M.D, Manvali, G. S., Abdusalam, M. & Joubert, D. P. (2016). Structural stability and electronic properties of AgInS2 under pressure. Eur. Phys. J. B 89, 90.
8. Gonze, X., Beuken, J.M., Caracas, R., Detraux, F., Fuchs, M., Rignanese, G.M., … Allan, D.C. (2002). First-principles computation of material properties: the Abinit software project. Computational Materials Science, 25, 478-492. http://dx.doi.org/10.1016/S0927-0256(02)00325-7.
9. Gonze, X., Rignanese, G.M., Verstraete, M., Beuken, J.M., Pouillon, Y., Caracas, R., … Allan D. C. (2005). A brief Introduction to the Abinit software package. Z. Kristallogr, 220, 558-562.
10. Khudaye, I. H., Ali, B. H. H., Mustafa, M. H. & Ibrahim, A. J. (2018). Investigation of the structural, optical and electrical properties of $AgInSe_2$ thin films. Ibn Al-hartham Journal. for pure and Appl. Sci., 31.
11. Koitabashi, K., Ozaki, S. & Adachi, S. (2010). Optical properties of single crystalline chalcopyrite semiconductor $AgInSe_2$. J. Appl. Phys., 107, 053516.
12. Kopytov, A. V. and Kosobutsky, A. V. (2010). Thermodynamic and elastic properties of $AgInSe_2$ and $AgInTe_2$. Phys. Solid State, 52, p1359–1361. https://doi.org/10.1134/S1063783410070061.
13. Kopytov, A.V. & Kosobutsky, A.V. (2010). Thermodynamic and elastic properties of $AgInSe_2$ and $AgInTe_2$, *Phys.* Solid State, 52, 1359–1361. https://doi.org/10.1134/S1063783410070061.
14. Kotmool, K., Bovornratanaraks, T. & Yoodee, K. (2015). Ab initio study of structural phase transformations and band gap of chalcopyrite phase in AgInTe2 under high pressure, Solid State Communication, 220, 25-30. https://doi.org/10.1016/j.ssc.2015.07.002.
15. Kulkarni, H. R. (2016). Characterization and optical properties of $AgInSe_2$ thin films prepared by electrodeposition technique. Int. Res. Jou. of management Sci. and Tech, 7, 197-204.
16. Lee, J. J., Lee, J. D., Ahn, B. Y., Kim, S. H. & Kim, K. H. (2007). Structural and optical properties of AgInSe2 films prepared on Indium Tin Oxide substrates. J. Kor. Phys. Soc., 50, 1099-1103.
17. Madelung, O. (2004). Semiconductors: Data Handbook, New York, Springer, 3rd edition, pp 293.
18. Martins, P. & Pamela, A. (2005). Growth and characterization of Epitaxial Silver Indium diselenide. url: http://hdl.handle.net/2142/88003.
19. Mustafa, H., Hunter, D., Pradhan, A. K., Roy, U. N., Cui, Y. & Burger, A. (2007) Synthesis and characterization of $AgInSe_2$ for application in thin film solar cells. Thin Solid films 515, 7001-7004.
20. Ranjbar, M., Tahor, M. A. & Sadeghinia, M. (2014). A facile route to synthesis of $AgInS_2$ nanostructures, Bull. Mater. Sci., vol. 37, No. 4, pp 767-772.
21. Santhosh, K. M. C. &Pradeep, B. (2009). Effect of H+ irradiation on the optical properties of vacuum evaporated $AgInSe_2$ thin film. Appl. Surf. Sci., 255, 8324-8327.

22. Sharma, S., Verma, A.S. & Jindal, V. k. (2014). First principles studies of structural, electronic, optical, elastic and thermal properties of Ag-chalcopyrites ($AgInX_2$: X=S, Se). Phys B: Cond. Matter, 438, 97-108. https://doi.org/10.1016/j.physb.2013.12.031
23. Tadjarodi, A. and Cheshmekhavar, A. H. (2012). Preparation of Silver Indium Sulfide Nanorods by facile microwave approach. MDPI, 16th inter. Conf. on synthetic organic Chemistry. DOI: 10.3390/ecsoc-16-01127.
24. Xue, D., Betzler K. & Hess, H. (2000). Dielectric properties of I-III-VI_2 type Chalcopyrite semiconductors. Phys. Rev., B 62, 13546. https://doi.org/10.1103/PhysRevB.62.13546
25. Yamada, K., Hoshino, N. & Nakada, T. (2007). Crystallographic and electrical properties of wide gap $Ag(In_{1-x}\ Ge_x)Se_2$ thin films and solar cells. Sci Technol. Adv. Mater, 7, 42-45.
26. Yin, J., Jia J. & Yi, G. (2013). Synthesis and photoelectric application of $AgInS_2$ clusters. Mater. Lett., 111, 85-88. https://doi.org/10.1016/j.matlet.2013.08.070.
27. Yoshino, K., Mitani, N. & Ikari, T. (2001). Optical and electrical properties of $AgIn(SSe)_2$ crystals. Phys,B: Cond. Matter 302-303, 349-356.
28. Zhanga, S. R., Xie, I. H., Chen, X. W., Shi, Z. G. & Song, K. H. (2014). Theoretical study of the structural and thermal properties of chalcopyrite structure $AgInTe_2$, Chalcogenide. Letters, 11, 373 -379.